DOI: 10.1002/ejic.201000795

Cuboidal Mo_3S_4 and Mo_3NiS_4 Complexes Bearing Dithiophosphates and Chiral Carboxylate Ligands: Synthesis, Crystal Structure and Fluxionality

Rita Hernandez-Molina,*[a] Javier Gonzalez-Platas,[b] Konstantin A. Kovalenko,[c,d] Maxim N. Sokolov,[c,d] Alexandre V. Virovets,[c,d] Rosa Llusar,[e] and Cristian Vicent*[f]

Keywords: Clusters / Phosphorus / Molybdenum / Nickel / X-ray diffraction / NMR spectroscopy

New triangular Mo and W cluster complexes incorporating (*S*)-lactic acid (HLac), $[Mo_3S_4(\mu\text{-Lac})(dtp)_3(py)]$ (**1**) and $[W_3S_4(\mu\text{-Lac})(dtp)_3(py)]$ (**2**), were prepared [dtp = $(EtO)_2PS_2$]. Analogous synthetic procedures were adapted for the synthesis of cuboidal Mo_3NiS_4 to yield $[Mo_3(Nipy)S_4(py)(\mu\text{-OAc})(dtp)_3(py)]$ (**3**). The crystal structures of **1** and **3** were determined. A detailed variable-temperature $^{31}P\{^1H\}$ and ^1H NMR study of compounds **1** and **3** indicated fluxional behaviour in non-coordinating solvents ($CDCl_3$, CD_2Cl_2 and $CDCl_2CDCl_2$). A number of dynamic processes were identified involving the Mo–py site that include configuration inversion [(*P*) to (*M*)], hindered Mo–N rotation and pyridine exchange. Experiments with deuterated pyridine revealed a faster substitutional lability of Mo–py compared with Ni–py.

Introduction

The easily available complexes of triangular chalcogenido-bridged clusters $[M_3(\mu_3\text{-}Q)(\mu\text{-}Q)_3]^{4+}$ (M = Mo, W; Q = S, Se) are excellent starting materials for heterometallic cuboidal clusters. The M_3Q_4 cores act as metalloligands towards transition or post-transition metal atoms (M′) in a low oxidation state to afford heterodimetallic $Mo_3M'S_4$ clusters.[1] Such heterometallic clusters are attracting considerable attention, because they show catalytic activity in a wide range of reactions including the addition of alcohols and carboxylic acids to electrophilic alkynes, cyclopropanation reactions and N–N bond cleavage.[2–6] The most studied are the aqua complexes and complexes with diphosphanes, cyclopentadienyl groups and dithiophosphates.[7] The most extensively studied are the aqua complexes, for which the incorporation of more than 20 different heterometals has been achieved.[8] A serious drawback here is that a very high acidity has to be maintained to prevent hydrolysis (the water molecules coordinated to Mo or W in the cluster show high Brønsted acidity), which limits the scope of possible applications of these complexes. The cyclopentadienyl derivatives offer the possibility of completely blocking competing reactivity at Mo or W sites.[9,10] Complexes with diphosphanes are known for Sn,[11] Cu,[2,12] Ni,[13] Pd[14] and Co.[15,16] In particular, the $[Mo_3(CuCl)S_4(diphosphane)_3Cl_3]^+$ cluster complexes are efficient catalysts for the intramolecular cyclopropanation of 1-diazo-5-hexen-2-one and for the intermolecular cyclopropanation of alkenes such as styrene and 2-phenylpropene with ethyl diazoacetate.[2] The mode of coordination of dithiophosphates, $(RO)_2PS_2^-$ (dtp), is similar to that of diphosphanes, which thus can lead to various complexes of the type $[M_3Q_4(dtp)_3L_3]^+$ in which L is a neutral donor such as pyridine (py).[7,17] More often the dtp complexes are prepared as carboxylates, $[M_3Q_4(dtp)_3(\mu\text{-RCOO})L]$, in which a bridging carboxylate group occupies the sites of two monodentate neutral donors (L), as illustrated in Scheme 1 (the ethoxy groups of dtp are omitted for clarity) for the series of structurally characterized complexes $[M_3Q_4(dtp)_3(\mu\text{-RCOO})(py)]$ (R = *p*-$O_2NC_6H_4$, CH_3, *p*-ClC_6H_4, $ClCH_2$ and Cl_3C) and their cuboidal analogues.[18–24]

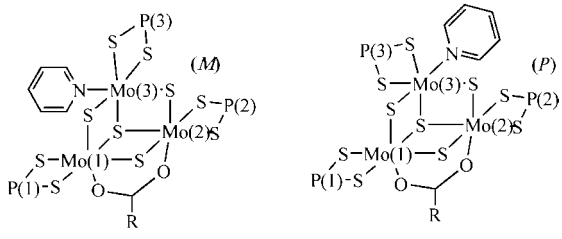

R = *p*-$O_2NC_6H_4$, CH_3, *p*-ClC_6H_4, $ClCH_2$, Cl_3C
R = CH_3CHOH (**1**)

Scheme 1.

[a] Dpto de Química Inorgánica, Facultad de Química, Universidad de La Laguna, 38200 La Laguna, Tenerife, Spain
[b] Dpto Física Fundamental II, Servicio de Difracción de Rayos X, Universidad de La Laguna, Tenerife, Spain
[c] A. V. Nikolayev Institute of Inorganic Chemistry SB RAS, Prospekt Lavrentyeva 3, 630090 Novosibirsk, Russia
[d] Novosibirsk State University, ul. Pirogova 2, 630090 Novosibirsk, Russia
[e] Departament de Química Física i Analítica, Universitat Jaume I, Av. Sos Baynat s/n, 12071 Castelló, Spain
[f] Serveis Centrals d'Instrumentació Científica, Universitat Jaume I, Avda. Sos Baynat s/n, 12071 Castelló, Spain
Supporting information for this article is available on the WWW under http://dx.doi.org/10.1002/ejic.201000795.

However, although the incorporation of the $d^{10}s^2$ metals (Zn^0, Cd^0, Sn^{II}, Pb^{II}, Sb^{III} and Bi^{III}) into the dithiophosphate cluster complexes has been extensively studied,[25,26] of all the transition metals only Cu^I has been incorporated.[27,28] A common structural feature of these clusters is a strong preference for the position *trans* to the capping μ_3-S atom to be occupied by one sulfur atom from the dtp ligand, whereas the pyridine molecule occupies the position *cis* to the μ_3-S atom and *trans* to the μ_2-S atom (Scheme 1). This mutual arrangement of a bidentate and a monodentate ligand is also common to diphosphane ligands coordinated to M_3Q_4 clusters and inherently furnishes chirality at the Mo(3) site. The absolute configurations of the resulting complexes can be described by (*P*) and (*M*) descriptors, which refer to the distinct orientation of the pyridine ligand coordinated to Mo(3) by keeping the μ_3-S atom behind the Mo_3 plane. However, the non-stereospecificity of the synthetic procedures (ligand substitution in the non-chiral Mo_3S_4 precursors) results in the formation of racemic mixtures, unless a chiral auxiliary ligand is provided. In this sense, the coordination of a chiral carboxylic acid, such as naturally occurring (*S*)-lactic acid, [$CH_3CH(OH)COOH$, HLac, also called L-lactic acid] provides a new way of introducing chirality into the clusters which in turn would yield a pair of diastereoisomers, namely (*PS*) and (*MS*). Herein we report the synthesis and characterization of new complexes with chiral (*S*)-lactate ligands, $[Mo_3S_4(dtp)_3(S\text{-}Lac)(py)]$ (**1**) and $[W_3S_4(dtp)_3(S\text{-}Lac)(py)]$ (**2**), and the first dtp complex with the $Mo_3NiS_4^{4+}$ core, $[Mo_3S_4(Nipy)(dtp)_3(OAc)(py)]$ (OAc = CH_3COO) (**3**). Multinuclear variable-temperature ^1H and $^{31}P\{^1H\}$ NMR spectroscopy allowed us to identify a number of dynamic processes that include configurational [(*P*) to (*M*)] inversion at the Mo(3) site, hindered rotation around the Mo–N bond and pyridine exchange at the Mo(3) site.

Results and Discussion

Synthesis and ESI-MS Characterization

The synthesis of **1**–**3** from the corresponding aqua complexes is straightforward and followed the established procedures.[29] The yields were close to quantitative. Sample solutions proved to be stable for days in low-coordinating solvents such as $CHCl_3$ or CH_2Cl_2. The ESI(+) mass spectra of **1**–**3** were recorded in CH_2Cl_2 in the presence of traces of NaI. The base peak corresponds to the species of general formula $[M - carboxylate - py]^+$ that is formed from the starting M compounds as a result of carboxylate dissociation accompanied by the release of a pyridine molecule. Additional species assigned to sodium adducts $[M + Na - py]^+$ are also observed. The addition of sodium salts proved to be crucial in the present case for promoting the ionization of the intact cluster under ESI conditions.[30] Figure 1 exemplifies typical ESI(+) mass spectra of compounds **1** and **3** dissolved in CH_2Cl_2 in the presence of traces of methanolic solutions of NaI.

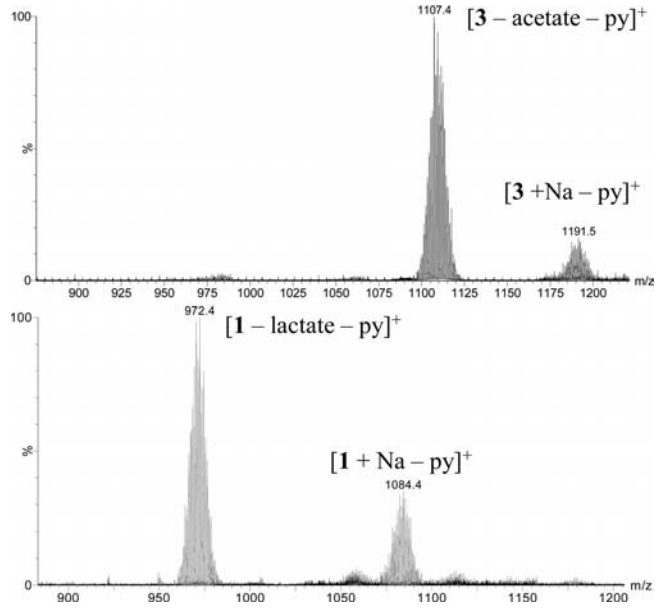

Figure 1. ESI mass spectra of compounds **1** and **3** in CH_2Cl_2 in the presence of traces of NaI recorded at U_c = 10 V.

Note that pyridine loss is invariably observed in the ESI mass spectra, which reflects the loose coordination of pyridine molecules in compounds **1**–**3**. The lability of coordinated py in coordinating solvents has previously been reported for $[Mo_3S_4(dtp)_3(\mu\text{-}OAc)(py)]$.[19] Solutions of **1**–**3** in more coordinating solvents (CH_3CN, CH_3OH or dimethyl sulfoxide) undergo partial or complete pyridine replacement by solvent either at the Mo or Ni site (in the case of **3**) accompanied by cluster decomposition, after around 1 h, as judged by ESI(+)-MS.

Crystal Structures

Compounds **1** and **3** were characterized by X-ray structural analysis. The main geometric parameters of **1** and **3** are summarized in Tables 1 and 2. Two independent cluster units are found in the asymmetric unit in the crystal structure of **1**. In both cluster entities, the cluster core in **1** reveals a distorted Mo_3 triangle, which is typical of an incomplete ligand environment in cuboidal clusters $Mo_3S_4^{4+}$ (see Figure 2). Lactato-bridging coordination produces a distortion of one Mo–Mo bond, which is contracted to 2.69 Å in contrast to 2.74–2.75 Å for the two non-bridged bonds. This geometry is typical of carboxylates of this type. The bridging lactato ligand is coordinated almost symmetrically [Mo(1)–O(1) 2.242(5) Å, Mo(2)–O(2) 2.253(5) Å]. A rather long Mo–N distance, 2.367(5) Å, is indicative of a rather loose coordination of this ligand, in agreement with previous findings {e.g., in $[Mo_3Se_4(dtp)_3(\mu\text{-}CH_3COO)(py)]$ the Mo–N distance is 2.377(7) Å}[29] and with the notable lability of the py ligand as evidenced by ESI mass spectrometry. In $[Mo_3S_4Cl_4(py)_5]$ and $[Mo_3S_4Cl_3(py)_6]I$ the Mo–N bonds are shorter, ranging from 2.28 to 2.33 Å.[31] The lactato oxygen atoms and the nitrogen atom of the py ligand

are coordinated *cis* to the μ_3-S capping atom. The three dtp ligands form four-membered chelate rings with one S atom occupying the *cis* and the other the *trans* position with regard to the capping sulfido atom, with no significant differences in the Mo–S bond lengths between them. This ligand arrangement is also found in other carboxylato complexes such as $[W_3S_4(dtp)_3(\mu\text{-}CH_3COO)(py)]$[18] and $[Mo_3Se_4(dtp)_3(\mu\text{-}CH_3COO)(py)]$.[29]

Table 1. Selected bond lengths [Å] for **1**.

Compound **1**			
Mo(1)–Mo(2)	2.6937(7)	Mo(4)–Mo(5)	2.6948(7)
Mo(1)–Mo(3)	2.7491(8)	Mo(4)–Mo(6)	2.7678(7)
Mo(1)–S(1)	2.3396(18)	Mo(4)–S(5)	2.3312(16)
Mo(1)–S(2)	2.2921(17)	Mo(4)–S(6)	2.2911(19)
Mo(1)–S(3)	2.2905(19)	Mo(4)–S(8)	2.2864(17)
Mo(1)–S(11)	2.5296(19)	Mo(4)–S(41)	2.5631(18)
Mo(1)–S(12)	2.566(2)	Mo(4)–S(42)	2.524(2)
Mo(1)–O(1)	2.243(5)	Mo(4)–O(3)	2.250(5)
Mo(2)–Mo(3)	2.7608(7)	Mo(5)–Mo(6)	2.7495(8)
Mo(2)–S(1)	2.3347(16)	Mo(5)–S(5)	2.3354(18)
Mo(2)–S(2)	2.2915(19)	Mo(5)–S(6)	2.2993(17)
Mo(2)–S(4)	2.2854(17)	Mo(5)–S(7)	2.2892(18)
Mo(2)–S(21)	2.5491(18)	Mo(5)–S(51)	2.5250(18)
Mo(2)–S(22)	2.531(2)	Mo(5)–S(52)	2.569(2)
Mo(2)–O(2)	2.253(5)	Mo(5)–O(4)	2.238(5)
Mo(3)–S(1)	2.3326(17)	Mo(6)–S(5)	2.3385(17)
Mo(3)–S(3)	2.2973(17)	Mo(6)–S(7)	2.2936(17)
Mo(3)–S(4)	2.2926(15)	Mo(6)–S(8)	2.2952(16)
Mo(3)–N(1)	2.367(5)	Mo(6)–N(2)	2.351(5)
Mo(3)–S(31)	2.5682(19)	Mo(6)–S(61)	2.5557(19)
Mo(3)–S(32)	2.5470(19)	Mo(6)–S(62)	2.5724(18)

Compound **3** can be described as resulting from the addition of the {Ni–py} fragment to the acetato analogue of **1**. This does not change the mutual orientation of the dtp, carboxylato and py ligands in the Mo_3S_4 moiety. As expected,[32,33] Ni incorporation somewhat lengthens the Mo–Mo bonds, but the strong overall asymmetry of the Mo_3 face persists because of the carboxylato bridge (see Table 2). The Ni–Mo and Mo–Mo (unbridged) bond lengths are typical of $Mo_3NiS_4^{4+}$ clusters.[9,10,13,32,33] The Ni–py bond is

Table 2. Selected bond lengths [Å] for **3**.

Compound **3**			
Mo(1)–Mo(2)	2.6901(6)	Mo(2)–S(10)	2.5369(16)
Mo(1)–Mo(3)	2.7714(6)	Mo(2)–S(11)	2.5717(18)
Mo(1)–Ni(1)	2.6959(8)	Mo(2)–O(1)	2.224(4)
Mo(1)–S(2)	2.3673(15)	Mo(3)–Ni(1)	2.6626(8)
Mo(1)–S(3)	2.3477(14)	Mo(3)–S(1)	2.3465(14)
Mo(1)–S(4)	2.3537(14)	Mo(3)–S(3)	2.3446(14)
Mo(1)–S(30)	2.5394(17)	Mo(3)–S(4)	2.3503(14)
Mo(1)–S(31)	2.5682(17)	Mo(3)–S(20)	2.5821(18)
Mo(1)–O(2)	2.205(4)	Mo(3)–S(21)	2.5698(17)
Mo(2)–Mo(3)	2.7917(7)	Mo(3)–N(1)	2.361(5)
Mo(2)–Ni(1)	2.6863(8)	Ni(1)–S(1)	2.2012(15)
Mo(2)–S(1)	2.3374(14)	Ni(1)–S(2)	2.1778(15)
Mo(2)–S(2)	2.3622(15)	Ni(1)–S(4)	2.2061(15)
Mo(2)–S(3)	2.3411(14)	Ni(1)–N(2)	1.956(5)

short [1.956(5) Å] in **3**; this value is close to that observed in $[\{Mo_3NiS_4Cp'_3\}_2(\mu\text{-}4,4'\text{-bipy})]^{2+}$ [1.937(4) Å; Cp′ = η^5-C_5H_4Me].

Variable-Temperature $^{31}P\{^1H\}$ and ^1H NMR Studies

We performed variable-temperature (VT) $^{31}P\{^1H\}$ and ^1H NMR experiments on **1** and **3** in weakly coordinating solvents to probe their structural integrity in solution. As can be inferred above from Scheme 1, the complexes $[M_3Q_4(dtp)_3(\mu\text{-}RCOO)(py)]$[13] possess overall C_1 symmetry, and consequently none of the Mo sites [and therefore the phosphorus atoms P(1), P(2) and P(3)] are equivalent. On the basis of this C_1 symmetry, one should expect three ^{31}P resonances for the $[M_3Q_4(dtp)_3(\mu\text{-}RCOO)(py)]$ series, but only two phosphorus resonances are observed in the $^{31}P\{^1H\}$ NMR spectra recorded close to room temperature, whereas upon cooling the three expected resonances appear in agreement with the structure determined in the solid state.[34,35] The most widely accepted explanation for this dynamic process is that dissociation of the loosely coordinated pyridine molecule at the Mo(3) site causes the P(1)

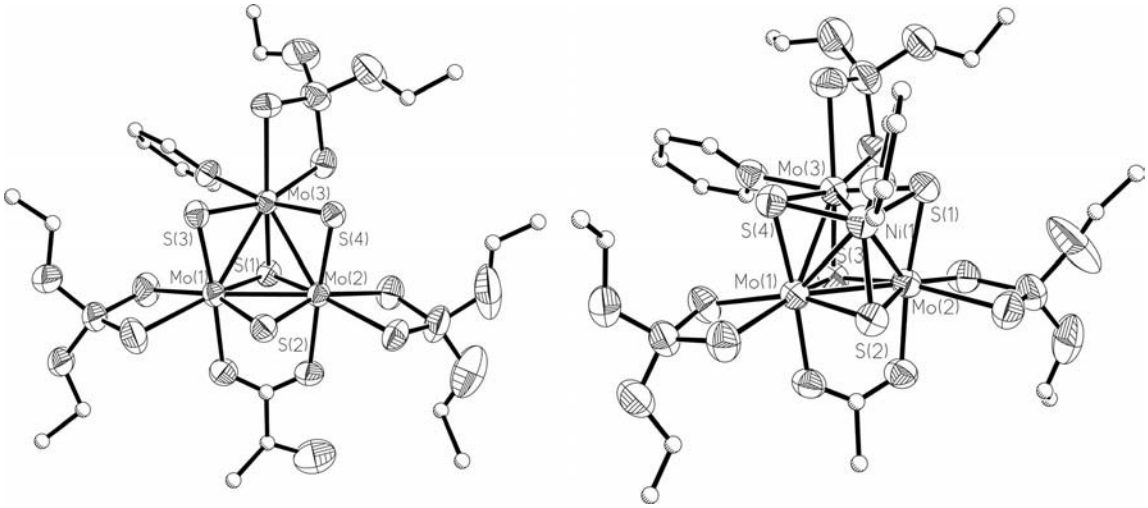

Figure 2. ORTEP representations (50% probability ellipsoids) of compounds **1** and **3**. Carbon atoms are drawn as spheres for clarity.

and P(2) resonances to coalesce.[34,35] In this work we investigated the fluxionality of **1**–**3** by VT $^{31}P\{^{1}H\}$ and ^{1}H NMR in the range T = –90 to 110 °C. We describe here in detail VT multinuclear NMR spectra for **1** and **3**, which feature non-chiral and chiral carboxylato-bridging ligands, respectively, as representative for the two series of compounds.

Fluxionality in [Mo$_3$(Nipy)S$_4$(EtOdtp)$_3$(μ-CH$_3$COO)(py)] (3)

The $^{31}P\{^{1}H\}$ NMR spectra at low temperature (typically from T = –55 to –30 °C) display three narrow resonances (at δ = 111.10, 110.89 and 110.74 ppm) of approximately equal intensity, a pattern consistent with the structural non-equivalence of the three dtp ligands. Figure 3 shows the $^{31}P\{^{1}H\}$ NMR spectra of compound **3** in $CDCl_3$ as the temperature is raised from –50 to 30 °C.

As can be seen, the two downfield resonances broaden and eventually coalesce at $T_C \approx -7$ °C ($\Delta G^{\neq}_{-7\,°C}$ = 12.6 kcal mol^{-1}) to an averaged peak. At 10 °C only two resonances at δ = 111.03 and 110.28 ppm are observed in an approximate 2:1 ratio. On the basis of the relative intensities and temperature-dependent behaviour of the phosphorus resonances and previously reported data,[34,35] the two resonances at lower field have been assigned to the two chelate [P(1) and P(2)] dtp ligands coordinated to Mo(1) and Mo(2) and the remaining one to the dtp ligand coordinated to Mo(3) (see Figure 3). In CD_2Cl_2, an identical T_C value ($T_C \approx -7$ °C) is observed, and the VT $^{31}P\{^{1}H\}$ NMR spectra remain unchanged in the range T = –30 to –90 °C. The above observations point to a dynamic process that renders the P(1) and P(2) atoms equivalent as a result of rapid exchange between two closely related structures. The P(3) resonance as well as resonances of the hydrogen atoms from the Mo–py group (see below) remain unaffected upon this interconversion. We hypothesize that species **3a** and **3b** interconvert through an inversion at the chirotopic Mo(3) centre according to Scheme 2.

Several mechanisms for the inversion of **3a** to **3b** at the chirotopic Mo(3) centre are feasible. On the one hand, interconversion may take place through a sequence that involves dissociation of the pyridine molecule from the Mo(3) site, inversion of the four-membered metallacycle defined by the dtp ligand attached to the Mo(3) and reassociation of the pyridine ligand according to pathway a depicted in Scheme 2. This mechanism is likely to be non-operative, because the characteristic variable-temperature $^{31}P\{^{1}H\}$ NMR spectra of compound **3** remain largely unchanged on addition of various amounts of pyridine. Moreover, ^{1}H resonances from the Mo–py group did not display dynamic behaviour in the absence of added pyridine (see discussion of the ^{1}H NMR spectra below). On the other hand, the hemilability of the dtp ligand at the Mo(3) site (dissociation/reassociation of one of the S termini of the chelating ligand) seems to be the preferred operative process (see pathway b), which allows fast pyridine migration at the Mo(3) site and makes Mo(1) and Mo(2), and accordingly P(1) and P(2), equivalent. The hemilability of the dtp ligands[36] in metal complexes is well established. An analogous mechanism based on diphosphane hemilability has previously been observed for the epimerization of the closely related cluster $[Mo_3S_4Cl_3(dppe)_3]^+$.[37]

To gain further insight into these dynamic processes we undertook a VT ^{1}H NMR study of **3**. Similarly to the $^{31}P\{^{1}H\}$ NMR spectra, the ^{1}H NMR spectra are strongly broadened at close to room temperature, and well-resolved signals appear below –20 °C (Figure S1). The ^{1}H NMR spectra in the aliphatic region provide only limited structural information because of the extensive overlapping of the potentially six non-equivalent OCH_2CH_3 groups of the

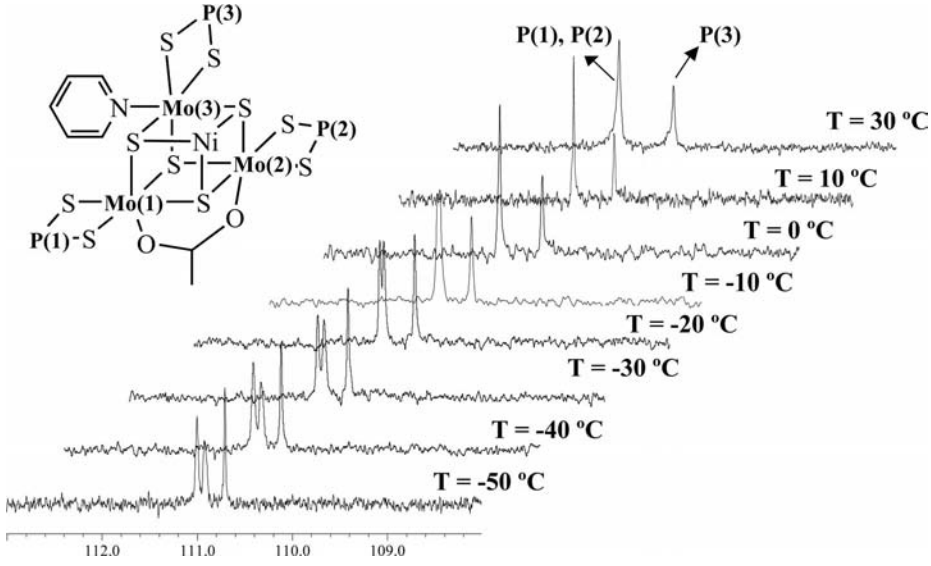

Figure 3. Variable-temperature $^{31}P\{^{1}H\}$ NMR spectra of **3** in $CDCl_3$. A schematic view of compound **3** is also included with OCH_2CH_3 and Ni–py omitted for clarity.

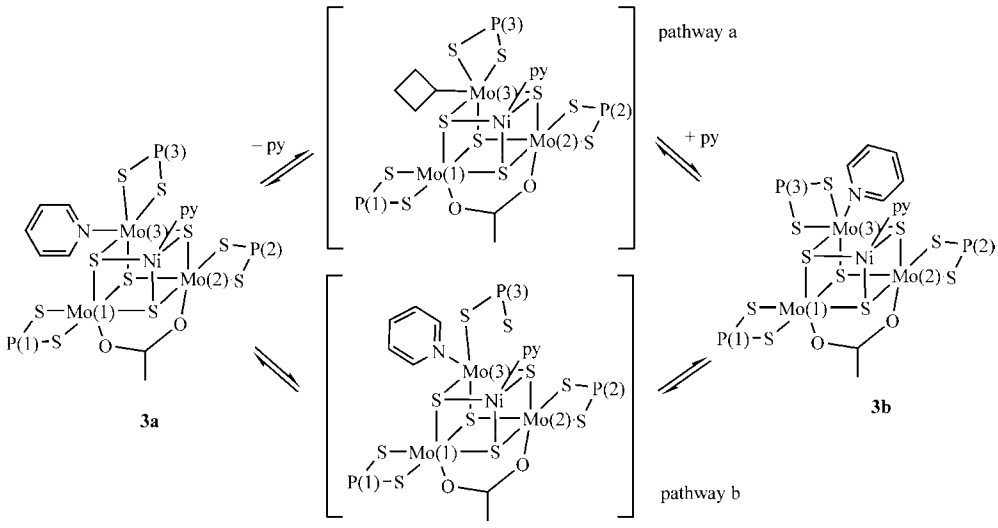

Scheme 2.

three dtp ligands. All attempts to assign different signals to the OCH_2CH_3 groups of the dtp ligands were unsuccessful. A combination of ^1H–^1H COSY and single-bond ^1H–^{13}C HSQC experiments revealed that signals in the δ = 3–4.5 ppm range are assignable to both CH_2 and CH_3 groups, and those in the δ = 0.7–2 ppm range correspond to the CH_3 groups of both OCH_2CH_3 and CH_3COO groups. Line-selective irradiation experiments also failed to provide satisfactory NOE effects to neighbouring protons as evidence of their correct assignment. In the aromatic region, two different pyridine molecules are readily identified at T = 20 °C, one of them displaying narrower proton resonances than the other one, whereas at –20 °C both pyridine ligands give narrow signals (see Figure 4a). The set of narrower signals at room temperature was assigned to the Ni–py moiety, which indicates an inherently lower lability than that of the Mo–py group. ^1H–^1H COSY experiments further confirmed this assignment (see Figure 4b).

As far as the fluxionality of **3** is concerned, VT ^1H NMR proton resonances of the Mo–py ligand reveal an additional dynamic process at low temperature. Upon cooling $CDCl_3$ solutions of **3** from –30 to –55 °C, all the aromatic resonances in the ^1H NMR spectra remain largely unchanged except for the lowest-field signal corresponding to the *o*-H hydrogen atom of the Mo–py unit. Decoalescence of the *o*-H signal is reached at –46 °C in $CDCl_3$ solution, and below this temperature two *o*-H resonances of the Mo–py ligand are observed in a 1.0:1.0 ratio, although the slow-limit regime was not reached below –55 °C. The ^1H NMR experiments were therefore extended down to T = –90 °C in CD_2Cl_2, which allowed us to reach the slow-limit regime at around –70 °C [δ = 9.15 (d), 9.31 (d) ppm]. These signals were assigned to the isolated *o*-H pyridine proton of different conformers on the basis of chemical shift, multiplicity and intensity. Irradiation of the resonance with δ = 9.15 ppm resulted in saturation transfer to the resonance at δ = 9.31 ppm, which verifies that the two protons are exchange partners. From T_C = –46 °C and the $\Delta\nu$ values in the slow-limit regime observed in CD_2Cl_2, the activation free energy was estimated to be $\Delta G^{\neq}_{-46\,°C}$ = 11.0 kcal mol^{-1}, which indicates that it is a dynamic process disconnected from the isomerization manifested in the VT ^{31}P NMR ex-

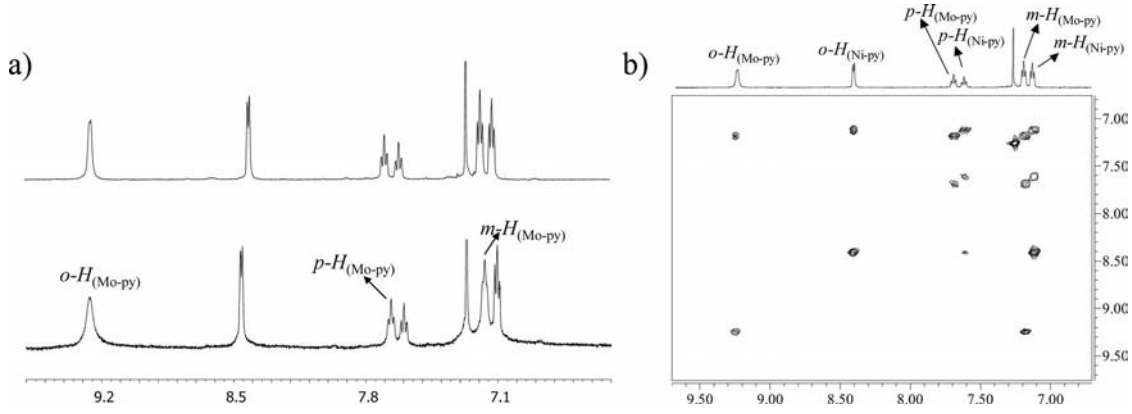

Figure 4. (a) ^1H NMR spectra in the aromatic region of $CDCl_3$ solutions of compound **3** at T = 20 (bottom) and –20 °C (top); (b) COSY spectrum of **3** in the aromatic region recorded at T = –20 °C.

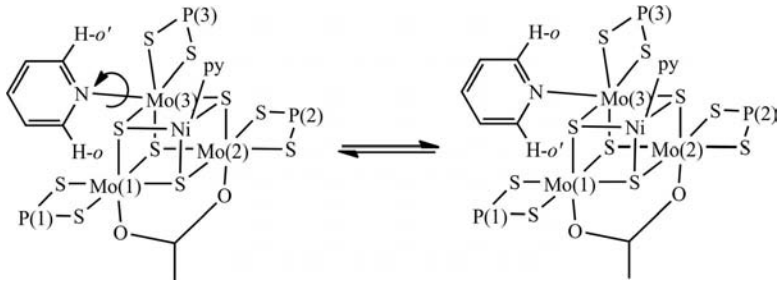

Scheme 3.

periments. This VT NMR behaviour is consistent with a dynamic process based on a restricted rotation about the Mo–N(pyridine) bond in **3**, as shown in Scheme 3.

Other plausible fluxional processes might be hapticity interconversion of pyridine molecules. For Ru^{II} complexes such as [$CpRu^{II}(\eta^6$-py)] and [$CpRu^{II}(\eta^1$-py)$(CH_3CN)_n$], this process has been observed to occur only in the coordinating solvent CD_3CN.[38,39] Given the lack of readily available coordination sites at the Mo site in compound **3**, it is unlikely that a similar reversible haptotropic shift of the coordinated pyridine ring could take place here. Enthalpic ($\Delta H^{\neq}$) and entropic ($\Delta S^{\neq}$) contributions to the free energy of activation of this process were obtained from Eyring plots. Representative experimental and simulated ^{1}H NMR spectra are shown in Figure S2.[40,41] Line-shape analysis gave $\Delta H^{\neq} = 12.1 \pm 0.2$ kcal mol^{-1} and $\Delta S^{\neq} = -4.9 \pm 0.2$ cal mol^{-1}. These values are comparable to those observed for the metal–pyridine rotational barriers observed in [$(\eta$-$C_9H_7)_2$Nb(H)(py)].[42]

Like the ^{31}P signals, the proton resonances of the Mo–py group progressively broaden on raising the temperature from 20 to 110 °C. In particular, the *o*-H resonance of the Mo–py moiety gradually broadens and is shifted upfield. This behaviour suggests an equilibrium between coordinated pyridine at the Mo(3) site and free pyridine, although signals of free pyridine are not observed at all in the $CDCl_2CDCl_2$ temperature window. Upon addition of pyridine, we observed that the ^{1}H resonances of the pyridine ligand attached to the Mo(3) site in **3** undergo facile exchange with free pyridine in the range $T = -10$ to 80 °C on the NMR timescale. Figure 5 shows the stacked VT NMR spectra of **3** in the presence of around a two-fold excess of pyridine.

Addition of free pyridine (ca. 0.5–2 equiv.) causes all these ^{1}H resonances, both for coordinated and free pyridine, to broaden (see Figure 5, upper trace) in the ^{1}H NMR spectrum of pure **3**. The line broadening of the proton resonances of the Mo–py group depends upon the amount of added pyridine at the same temperature, an observation consistent with a dynamic process of bimolecular nature, which most likely occurs by association of a second pyridine molecule at Mo(3) promoted by decoordination of one arm of the dithiophosphato ligand. Quantitative ^{1}H–^{1}H EXSY spectra[43] were recorded to gain deeper insights into the pyridine exchange process. Illustrative EXSY spectra that confirm mutual exchange between *o*-H and *m*-H signals in the coordinated and free pyridine are given in Figure S3. Upon addition of 1 and 2 equiv. of pyridine to $CDCl_3$ solutions of compound **3**, EXSY spectra were recorded, and from these experiments an array of rate constants at different temperatures (T = 10, 0, –10 °C) for two types of exchange couples (*o*-H and *m*-H signals) were obtained in accord with ref.[43] Significant information can be readily obtained; for example, rate constants for pyridine

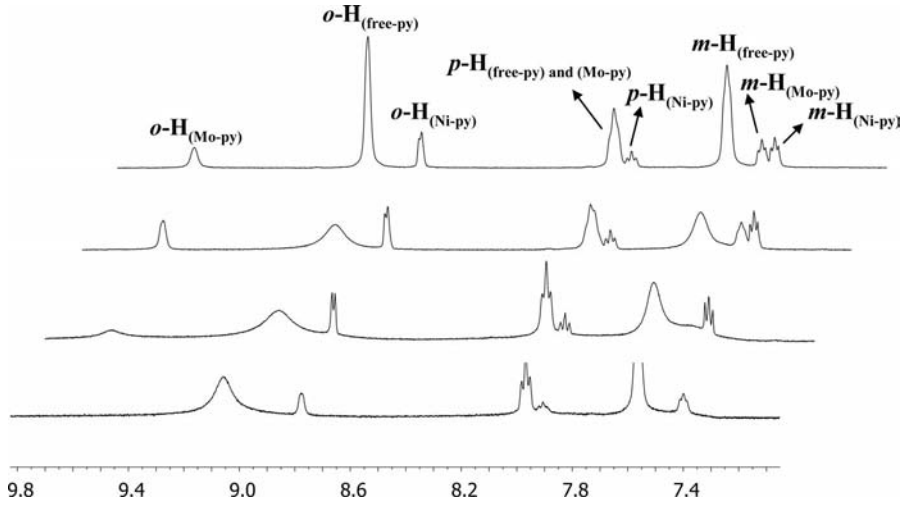

Figure 5. Variable-temperature (increments of 30 °C) ^{1}H NMR spectra in the range $T = -20$ (top) to 80 °C (bottom) of compound **3** in $CDCl_2CDCl_2$ in the presence of added pyridine.

exchange increased with increasing amounts of pyridine, consistent with a bimolecular dynamic process. Identical bimolecular pyridine exchange has been observed for [CpTi(BuN)Cl(py)] in the presence of added pyridine.[44] For closely related pyridine exchange processes, line-shape analysis or quantitative EXSY spectroscopy have proven to be very useful for obtaining a detailed insight into the intimate mechanistic picture of the process. For example, for palladium complexes featuring 2,2′-bipyridyl and substituted pyridine ligands of general formula $[Pd(bipy)(py)_2]^{2+}$ or $[Pt(bipy)(py)_2]^{2+}$, the mechanistic picture (dissociative exchange of hindered rotation-mediated pyridine exchange) of the pyridine exchange is dramatically affected by the identity of the substituent in the pyridine ligand and is associated with *syn*/*anti* inversion.[45–47]

Note the distinctive lability of the Mo(3)–py and Ni(1)–py groups, the latter being exchanged (on the NMR timescale) only at high T (typically $T > 90$ °C). In additional ^{1}H NMR experiments with an excess of C_5D_5N, immediate py replacement at the Mo(3) site takes place, whereas replacement at the Ni site is slower. This experimental evidence is in agreement with the increased lability of Mo–py relative to Ni–py, most likely due to the more congested environment around the Mo(3) site.

Fluxionality in [Mo$_3$S$_4$(dtp)$_3$(μ-Lac)(py)] (1)

Given the structural similarities between **1** and **3**, we expected to observe related fluxionality, that is (1) hindered Mo–N rotation at low temperature and (2) configurational inversion [(*P*) and (*M*)] at the Mo(3) site through a dissociative mechanism. However, besides the two possible configurations around the inherently stereogenic Mo(3) centre [(*P*) and (*M*) configurations], compound **1** contains a stereogenic carbon atom (*S*) in the lactato bridge, consequently, two invertomers are expected as a diastereomeric couple [(*PS*) and (*MS*); see Scheme 4].

Each diastereoisomer has three non-equivalent phosphorus atoms such that up to six different phosphorus resonances were expected in the low-temperature $^{31}P\{^1H\}$ NMR spectrum. In a similar way to that described above for **3**, the VT $^{31}P\{^1H\}$ NMR spectra of **1** provide crucial information for determining its integrity in solution and reveal the presence of several isomers. The VT $^{31}P\{^1H\}$ NMR spectra of $CDCl_3$ solutions of **1** are displayed in Figure 6.

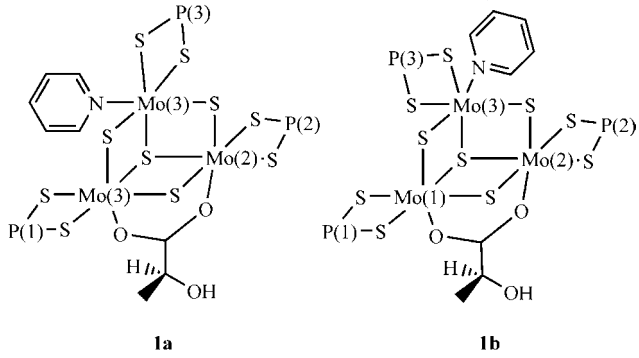

Scheme 4.

The $^{31}P\{^1H\}$ NMR spectrum at –40 °C reveals five dominant singlets, the one at δ = 110.83 ppm and those downfield at δ = 111.81, 111.75, 111.53 and 111.42 ppm with relative intensities of 2:1:1:1:1. The VT NMR spectra suggest the presence of an equally populated mixture of diastereoisomers **1a** and **1b**, each of them represented by two different singlets in the lower-field region of the spectra [those corresponding to P(1) and P(2), see Scheme 4], whereas the signal centred at δ = 110.83 ppm, which does not sense the weak magnetic difference provided by the lactato ligand, has been attributed to P(3) in both isomers. The UV/Vis circular dichroism spectra of CH_2Cl_2 or $CHCl_3$ solutions of **1** are silent at $\lambda > 300$ nm (which means the absence of chirality associated with the metal centres), which also furnishes definitive proof of the presence of species **1a** and **1b** in equal populations.

As far as the fluxionality of compound **1** is concerned, upon warming from T = –40 to 10 °C, the P(1) and P(2) resonances broaden and eventually coalesce near T = 0 °C, although, because of the presence of several overlapping resonances, it was difficult to determine T_C accurately. The similarities between $\Delta\nu$ for the P(1) and P(2) signals in the slow-limit regime together with coalescence temperatures similar to those found for **1** suggest that the exchange between P(1) and P(2) proceeds similarly to pathway b in

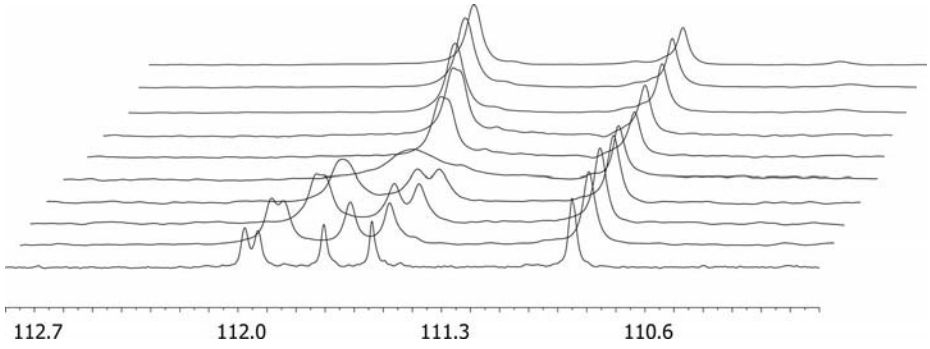

Figure 6. Variable-temperature (increments of 10 °C) $^{31}P\{^1H\}$ NMR spectra of **1** in $CDCl_3$ in the range T = –40 to 50 °C.

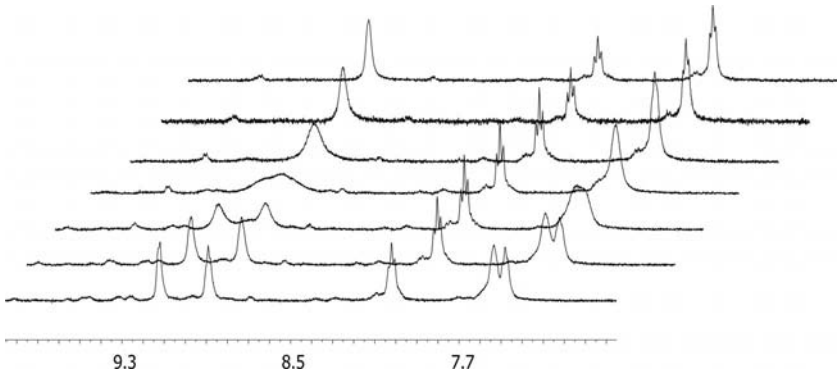

Figure 7. VT ^{1}H NMR spectra (increments of 10 °C) of **1** in the range T = –75 to –15 °C recorded in CD_2Cl_2.

Scheme 2, that is, interconversion between **1a** to **1b** involving hemilabile dtp ligands. Above 10 °C, only two resonances are observed in a 2:1 ratio, in agreement with a rapid (on the NMR timescale) interconversion of **1a** to **1b**.

The ^{1}H NMR spectrum of **1** in $CDCl_3$ is similar to that of **3**. In the aliphatic region the signals are not diagnostic of the molecular organization as a consequence of extensive peak-overlapping. The resonance pattern in the aromatic region is also quite simple despite the presence of two pairs of diastereoisomers. For the Mo–py moiety, three resonances are observed close to room temperature, which indicates that the distinctive chemical environments of the Mo–py moieties in **1a** and **1b** are not manifested in the ^{1}H NMR spectrum. Figure 7 shows the VT NMR spectra of compound **1** in CD_2Cl_2 in the range of T = –75 to –15 °C.

At low temperatures, the same types of decoalescence at –44 °C are observed in the ^{1}H NMR spectra of complex **1** as with **3**, with $\Delta G^{\neq}_{-44\,°C}$ = 10.7 kcal mol^{-1} for the *ortho*-protons [δ = 9.12 (d), 9.01 (d) ppm]. A significant difference in comparison with compound **3** is that the *meta*-hydrogen signals in **1** are also split at low temperature as a consequence of hindered Mo–py rotation. On heating to ambient temperature, the *o*-H and *m*-H resonances broaden and eventually coalesce into a time-averaged signal (see spectrum at T = –15 °C for *o*-H and T = –25 °C for *m*-H). Like **3**, this fluxional behaviour is consistent with the exchange of the non-equivalent *o*-H and *m*-H sites caused by hindered rotation of the pyridine ligand about the Mo–N bond axis. Activation parameters for this Mo–N_{py} rotation are virtually the same as in **3**, as expected from their structural similarities. From the line-shape analysis of the *o*-H and *p*-H resonances in **1**, averaged values of $\Delta H^{\neq}$ = 12.0 ± 0.2 kcal mol^{-1} and $\Delta S^{\neq}$ = –4.5 ± 0.2 cal mol^{-1} were estimated, which are similar to those obtained for **3**. ^{1}H NMR experiments were also conducted in the presence of pyridine to confirm that inversion at the Mo(3) site also occurs through a dissociative mechanism. Analogous exchange of *o*-H and *m*-H protons between pyridine coordinated to Mo and free pyridine evidences such a process for the interconversion of **1a** to **1b**, as illustrated in Figure S4, which confirms mutual exchange between *o*-H, *m*-H and *p*-H in the coordinated and free pyridine.

Conclusions

The synthetic procedures and electrospray ionization mass spectrometry characterization of a series of cubane-type Mo and W cluster complexes with M_3S_4 (M = Mo and W) and Mo_3S_4Ni cluster cores bearing dithiophosphato and carboxylato-bridging ligands of general formula $[Mo_3S_4(\mu\text{-Lac})(dtp)_3(py)]$ (**1**), $[W_3S_4(\mu\text{-Lac})(dtp)_3(py)]$ (**2**) and $[Mo_3(Nipy)S_4(\mu\text{-OAc})(dtp)_3(py)]$ (**3**) have been reported. Crystal structures of **1** and **3** were determined, confirming the gross connectivities in the Mo_3S_4 and Mo_3S_4Ni cluster cores. The bridging carboxylato ligand coordinates almost symmetrically in both structures, and a rather long Mo–N distance in the Mo–py unit is indicative of a rather loose coordination of this ligand. The variable-temperature $^{31}P\{^1H\}$ and ^{1}H NMR spectra of compounds **1** and **3** evidenced a number of dynamic processes including inversion of the configuration [(*P*) to (*M*)] at the Mo–py site involving hemilabile dtp ligands, hindered Mo–py rotation and pyridine exchange (on the NMR timescale) in the presence of added pyridine. NMR experiments in the presence of [D_5]pyridine also revealed the distinctive lability of Mo–py relative to Ni–py, with ligand substitution faster for Mo–py groups than for Ni–py. Identical fluxionality was observed for compound **1** in which the presence of equally populated pairs of invertomers (**1a/1b**) was observed, as judged by NMR and circular dichroism spectroscopy.

Experimental Section

General Procedures: All the experiments were carried out in air. The solvents were purified by standard procedures. Stock solutions of the aqua complexes $[M_3S_4(H_2O)_9]^{4+}$ (M = Mo, W)[48] and $[Mo_3(NiCl)S_4(H_2O)_9]^{3+}$ in 2 M HCl were prepared according to the published procedures.[49] Potassium diethyldithiophosphate (Kdtp) was prepared by dissolving P_4S_{10} in an excess of hot ethanol followed by neutralization with 4 equiv. of KOH, concentration of the reaction solution and recrystallization of the solid from acetone/diethyl ether to give a snow-white crystalline product. Other reagents [P_4S_{10}, pyridine, acetic acid, L-lactic acid (85% aqueous solution)] were commercial quality reagents (Aldrich) and were used as purchased. A Q-TOF I (quadrupole-hexapole time-of-flight) mass spectrometer with an orthogonal Z-spray-electrospray interface

(Micromass, Manchester, UK) was used. The drying and nebulizing gases were nitrogen at flow rates of 800 and 20 L h^{-1}, respectively. A few drops of an NaI solution (1×10^{-3} M) in methanol were added to sample solutions (approx. 5×10^{-5} M) in dichloromethane, and the resulting mixture was infused through a syringe pump directly into the interface at a flow rate of 10 μL min^{-1}. The temperature of the source block was set to 120 °C and the interface to 150 °C. A capillary voltage of 3.5 kV was used in the positive scan mode, and low values of the cone voltage (U_c = 10 V) were used to control the extent of fragmentation. The chemical composition of each peak was assigned by comparison of the isotopic experimental pattern with the theoretical by using the MassLynx 4.0 program. $^{31}P\{^1H\}$ NMR spectra were recorded with a Varian Mercury 300 MHz spectrometer equipped with a four-nucleus probe operating at 121.48 MHz for ^{31}P NMR. ^1H NMR spectra and two-dimensional gradient-enhanced ^1H–^1H COSY, ^1H–^{13}C HSQC, 1D NOESY and 2D EXSY (300 ms mixing time) spectra were recorded with a Varian 500 MHz (Unity INOVA) spectrometer equipped with a 5 mm dual broadband gradient probe by using standard sequences provided in the vnmrJ software.[50] ^{31}P NMR spectra were referenced externally by using H_3PO_4 (85% in D_2O) in a capillary taken to be at δ = 0.0 ppm. ^1H NMR chemical shifts were referenced internally to residual solvent resonances. Variable-temperature NMR spectra were recorded in the range –90 to 110 °C by using different solvents ($CDCl_3$, CD_2Cl_2 and $CDCl_2CDCl_2$). Line-shape analysis was carried out with the gNMR V4.1.0 program.[41] Activation parameters were obtained by least-squares fitting of suitable plots of the corresponding kinetic values obtained from line-shape analysis and the measured temperatures of the experimental spectra. IR spectra (4000–400 cm^{-1}) were recorded with an IFS-85 Bruker spectrometer, and elemental analyses were carried out with an Analizador Elemental CNHS FLASH EA 1112.

Synthesis of $[Mo_3S_4(\mu\text{-Lac})(dtp)_3(py)]$ (1): Solid Kdtp (583 mg, 2.60 mmol) was added to a stock solution (15 mL) of $[Mo_3S_4(H_2O)_9]^{4+}$ (43 mM, 0.64 mmol). A brown precipitate separated immediately, which was filtered and dried in air. The dry product was dissolved in CH_3CN (50 mL), and an 85% aqueous solution of L-lactic acid, pyridine and DMF (30 drops of each reagent) were added to the resulting brown solution. The solution was left to concentrate slowly in an open beaker. After 2 d, black crystals of **1** were collected. Yield: 275 mg (40%). IR: $\tilde{\nu}$ = 3502 (s), 2980 (s), 2930 (m), 2897 (m), 1745 (s), 1639 (s), 1601 (m), 1545 (m), 1442 (m), 1411 (s), 1371 (s), 1345 (m), 1223 (m), 1162 (m), 1127 (m), 1098 (s), 1057 (s), 1008 (s), 964 (s), 812 (s), 794 (s), 695 (w), 655 (m), 640 (m), 569 (s), 532 (m), 480 (w), 450 (w) cm^{-1}. $^{31}P\{^1H\}$ NMR ($CDCl_3$, 30 °C, 121.48 MHz): δ = 111.41, 110.83 ppm. MS (ESI, positive mode, CH_3CN): *m*/*z* = 971 $[Mo_3S_4(S_2P(OEt)_2)_3]^+$, 787 $[Mo_3S_4(S_2P(OEt)_2)_2]^+$. MS (ESI, CH_2Cl_2): *m*/*z* = 972.4 [**1** – acetate – py]$^+$, 1084.4 [**1** + Na – py]$^+$. $C_{20}H_{40}Mo_3NO_9P_3S_{10}$ (1138.85): calcd. C 21.07, H 3.22, N 1.23, S 28.09; found C 20.73, H 3.08, N 1.52, S 28.64.

$[W_3S_4(\mu\text{-Lac})(dtp)_3(py)]$ (2): This complex was prepared as green needles in a similar manner from a $[W_3S_4(H_2O)_9]^{4+}$ solution (15 mL, 16 mM, 0.23 mmol) and Kdtp (212 mg, 0.94 mmol). Yield (non-optimized): 65 mg (20%). IR: $\tilde{\nu}$ = 3421 (s), 2984 (s), 1745 (s), 1639 (s), 1603 (m), 1535 (s), 1454 (s), 1443 (s), 1414 (s), 1387 (s), 1348 (s), 1219 (m), 1130 (s), 1098 (m), 1044 (m), 1008 (s), 965 (s), 815 (m), 791 (m), 692 (s), 643 (m), 530 (s), 435 (s) cm^{-1}. $^{31}P\{^1H\}$ NMR ($CDCl_3$, –40 °C, 121.48 MHz): δ = 107.43, 106.85 ppm. MS (ESI, positive mode, CH_3CN): *m*/*z* = 1235.4 [**2** – lactate – py]$^+$. $C_{20}H_{40}NO_9P_3S_{10}W_3$ (1403.61): calcd. C 17.09, H 2.85, N 1.00, S 22.80; found C 17.62, H 2.80, N 1.13, S 23.10.

$[Mo_3(Nipy)S_4(dtp)_3(OAc)(py)]$ (3): An excess of potassium dithiophosphate was added to a solution of green $[Mo_3NiS_4(H_2O)_{10}]^{4+}$ (4 mM, 2 M HCl). A brown precipitate was filtered off. The latter was dissolved in acetonitrile to give a brown solution, then a few drops of acetic acid were added, and the colour turned slightly green. A few drops of pyridine and DMF were added. Crystals were separated after a few days. Yield (non-optimized): 120 mg (65%). $^{31}P\{^1H\}$ NMR ($CDCl_3$, –40 °C, 121.48 MHz): δ = 111.03, 110.28 ppm. MS (ESI, positive mode, CH_2Cl_2): *m*/*z* = 1109.6 [**3** – acetate – py]$^+$, 1195.1 [**3** + Na – py]$^+$. $C_{24}H_{43}Mo_3N_2NiO_8P_3S_{10}$ (1247.64): calcd. C 23.08, H 3.45, N 2.24, S 25.6; found C 23.20, H 3.42, N 2.46, S 25.1.

X-ray Crystallographic Study: The diffraction data were collected with a Bruker-Nonius KappaCCD diffractometer by using graph-

Table 3. Crystallography data for compounds **1** and **3**.

	1	**3**
Empirical formula	$C_{20}H_{39}Mo_3NO_9P_3S_{10}$	$C_{24}H_{43}Mo_3N_2NiO_8P_3S_{10}$
Formula mass	1138.85	1247.64
Crystal system	monoclinic	monoclinic
a [Å]	13.6240(7)	21.9040(15)
b [Å]	22.6060(13)	12.1550(9)
c [Å]	14.5985(7)	34.679(2)
α [°]	90	90
β [°]	104.573(2)	90.313(3)
γ [°]	90	90
V [Å^3]	4351.5(4)	9232.9(1)
T [K]	295(2)	293(2)
Space group	*P*21	*C*2/*c*
Z	4	8
μ(Mo-K_α) [mm^{-1}]	1.481	1.795
Flack parameter	–0.03(4)	–
Reflections collected	45110	64132
Unique reflections/R_{int}	31142/0.0201	11331/0.048
$R1$[a]/$wR2$[b]	R_1 = 0.0481, $wR2$ = 0.0966	R_1 = 0.0647, $wR2$ = 0.1648
$R1$[a]/$wR2$[b] (all data)	R_1 = 0.1139, $wR2$ = 0.1250	R_1 = 0.0858, $wR2$ = 0.1848
Residual ρ [e Å^{-3}]	1.873, –0.930	1.90, –2.33

[a] $R1 = \Sigma(||F_o| - |F_c||)/\Sigma F_o$. [b] $wR2 = \Sigma[w(F_o^2 - F_c^2)^2]/\Sigma[w(F_o^2)^2]^{1/2}$.

ite-monochromated Mo-K_α radiation (λ = 0.71073 Å) with ϕ and ω scans chosen to give a complete asymmetric unit with the COLLECT program.[51] Denzo SMN and HKL2000 programs were used for indexed and scaled data.[52] The absorption correction was applied by using a semiempirical method based on multiple scanned reflections in the PLATON program,[53] and the structures were solved by direct methods with the SIR2004 program[54] and refined with the SHELXL-97 program.[55] All non-hydrogen atoms were refined with anisotropic thermal parameters by using full-matrix least-squares procedures on F^2. Molecules of dtp present slight thermal disorder increases on terminal carbon atoms. The methyl H atoms were refined as rigid groups, which were allowed to rotate but not to tip with $U_{iso}(H) = 1.5U_{eq}(C)$. All other hydrogen atoms were allowed to ride on their parent atoms with $U_{iso}(H) = 1.2U_{eq}(C)$. Crystallographic data for complexes **1** and **3** are presented in Table 3. CCDC-782179 (for **1**) and -783681 (for **3**) contain the supplementary crystallographic data for this paper. These data can be obtained free of charge from The Cambridge Crystallographic Data Centre via www.ccdc.cam.ac.uk/data_request/cif.

Supporting Information (see footnote on the first page of this article): ^{1}H NMR spectra of **3** at T = 20 (bottom) and –20 °C (top) in $CDCl_3$ (Figure S1), aromatic *o*-H Mo–py region of the experimental (left) and simulated (right) VT NMR spectra of **3** (Figure S2) and illustrative ^{1}H–^{1}H EXSY spectra of compounds **1** and **3** in the aromatic region (Figures S3 and S4).

Acknowledgments

R. H. M thanks the Spanish Ministerio de Ciencia e Innovación for funding through project CTQ2009-14443-C02-02. R. L. and C. V. are grateful for the financial support of the Spanish Ministerio de Ciencia e Innovación (grant CTQ2008-02670), the Fundació Bancaixa-UJI (research project P1.1B2007-12) and the Generalitat Valenciana (ACOMP/2010/276). The authors also thank the Servei Central D'Instrumentació Cientifica (SCIC) of the Universitat Jaume I and the Servicios Generales de la Universidad de La Laguna for providing us with the mass spectrometry, NMR and X-ray facilities. M. S. is grateful to the Russian Foundation for Basic Research (09-03-00413), and J. G. P. acknowledges the Project MAT (2010-21270-C04-02).

[1] R. Llusar, S. Uriel, *Eur. J. Inorg. Chem.* **2003**, 1271–1290.
[2] M. Feliz, E. Guillamon, R. Llusar, C. Vicent, S. E. Stiriba, J. Perez-Prieto, M. Barberis, *Chem. Eur. J.* **2006**, *12*, 1486–1492.
[3] T. Wakabayashi, Y. Ishii, Y. Murata, M. Mizobe, M. Hidai, *Tetrahedron Lett.* **1995**, *36*, 5585–5588.
[4] T. Wakabayashi, Y. Ishii, K. Ishikawa, M. Hidai, *Angew. Chem. Int. Ed. Engl.* **1996**, *35*, 2123–2124.
[5] I. Takei, K. Wakebe, T. Suzuki, T. Enta, Y. Suzuki, M. Mizobe, M. Hidai, *Organometallics* **2003**, *22*, 4639–4641.
[6] I. Takei, K. Dohki, K. Kobayashi, T. Suzuki, M. Hidai, *Inorg. Chem.* **2005**, *44*, 3768–3770.
[7] M. N. Sokolov, V. P. Fedin in *Comprehensive Coordination Chemistry II*, vol. 4 (Eds.: J. A. McCleverty, T. J. Meyer), Elsevier, New York, **2003**, pp. 768–824.
[8] R. Hernandez-Molina, M. N. Sokolov, A. G. Sykes, *Acc. Chem. Res.* **2001**, *34*, 223–230.
[9] K. Herbst, M. Monari, M. Brorson, *Inorg. Chem.* **2002**, *41*, 1336–1338.
[10] K. Herbst, L. Dahlenburg, M. Brorson, *Inorg. Chem.* **2004**, *43*, 3327–3328.
[11] R. Hernandez-Molina, I. V. Kalinina, P. A. Abramov, M. N. Sokolov, A. V. Virovets, J. G. Platas, R. Llusar, V. Polo, C. Vicent, V. P. Fedin, *Inorg. Chem.* **2008**, *47*, 306–314.
[12] R. Llusar, S. Uriel, C. Vicent, *J. Chem. Soc., Dalton Trans.* **2001**, 2813–2818.
[13] M. Feliz, R. Llusar, S. Uriel, C. Vicent, M. Brorson, K. Herbst, *Polyhedron* **2005**, *24*, 1212–1220.
[14] A. G. Algarra, M. G. Basallote, M. Feliz, M. J. Fernandez-Trujillo, E. Guillamon, R. Llusar, C. Vicent, *Inorg. Chem.* **2006**, *45*, 5576–5584.
[15] M. Feliz, R. Llusar, S. Uriel, C. Vicent, E. Coronado, C. J. Gomez-Garcia, *Chem. Eur. J.* **2004**, *10*, 4308–4314.
[16] A. Alberola, R. Llusar, C. Vicent, J. Andres, V. Polo, C. J. Gomez-Garcia, *Inorg. Chem.* **2008**, *49*, 3661–3668.
[17] J.-Q. Huang, J.-L. Huang, M.-Y. Shang, S.-F. Lu, X.-T. Lin, Y.-H. Lin, M.-D. Huang, H.-H. Zhuang, J.-X. Lu, *Pure Appl. Chem.* **1988**, *60*, 1185–1192.
[18] Y. Zhang, H. Zhang, X. Wu, *Acta Crystallogr., Sect. C* **1989**, *45*, 1424–1426.
[19] S. Lu, J. Huan, M. Huang, J. Huang, *Huaxue Xuebao (Acta Chim. Sinica)* **1989**, *47*, 24–29.
[20] J. Hu, H. Zhuang, J. Huang, J. Huang, *Jiegou Huaxue (Chin. J. Struct. Chem.)* **1989**, *8*, 6–9.
[21] J. Xia, Y. Yao, L. Wu, X. Huang, J. Lu, *Acta Crystallogr., Sect. C* **1998**, *54*, 1612–1615.
[22] Y. Tang, Z. Li, L. Wu, Y. Qin, Y. Kang, Y. Yao, *Jiegou Huaxue (Chin. J. Struct. Chem.)* **2002**, *21*, 71–77.
[23] Y. H. Tang, Y. Y. Qin, L. Wu, Z. J. Li, Y. Kang, Y. G. Yao, *Polyhedron* **2001**, *20*, 2911–2916.
[24] Y. Y. Qin, Y. H. Tang, Y. Kang, Z. J. Li, R. F. Hu, J. K. Cheng, Y. H. Wen, Y. Yao, *J. Mol. Str.* **2004**, *707*, 235–239.
[25] S. Lu, J. Huang, X. Huang, Q. Wu, D. Wu, *Inorg. Chem.* **2000**, *39*, 5348–5353.
[26] S. Lu, J. Huang, R. Yu, X. Huang, Q. Wu, Y. Peng, J. Chen, Z. Huang, Y. Zheng, D. Wu, *Polyhedron* **2001**, *20*, 2339–2352.
[27] H. Zhang, Y. Zheng, X. Wu, J. Lu, *Inorg. Chim. Acta* **1989**, *156*, 277–280.
[28] Y. Zheng, H. Zhang, X. Wu, *Acta Crystallogr., Sect. C* **1989**, *45*, 1990–1992.
[29] R. Hernández-Molina, M. N. Sokolov, P. Nunez, A. Mederos, *J. Chem. Soc., Dalton Trans.* **2002**, 1072–1077.
[30] W. Henderson, B. K. Nicholson, L. J. McCaffrey, *Polyhedron* **1998**, *17*, 4291–4313.
[31] J. Mizutani, S. Yajima, H. Imoto, T. Saito, *Bull. Chem. Soc. Jpn.* **1998**, *71*, 631–636.
[32] T. Shibahara, H. Yamasaki, H. Akashi, T. Katayama, *Inorg. Chem.* **1991**, *30*, 2693–2699.
[33] T. Shibahara, G. Sakane, M. Maeyama, H. Kobashi, T. Yamamoto, T. Watase, *Inorg. Chim. Acta* **1996**, *251*, 207–225.
[34] S. Lu, J. Huang, Z. Huang, J. Huang, J. Lu, *Jiegou Huaxue (Chin. J. Struct. Chem)* **1990**, *9*, 116–120.
[35] Y. Yao, H. Akashi, G. Sakane, T. Shibahara, H. Ohtaki, *Inorg. Chem.* **1995**, *34*, 42–48.
[36] D. Dakternieks, H. Zhu, D. Masi, C. Mealli, *Inorg. Chem.* **1992**, *31*, 3601–3606.
[37] R. Frantz, E. Guillamon, J. Lacour, R. Llusar, V. Polo, C. Vicent, *Inorg. Chem.* **2007**, *46*, 10717–10723.
[38] R. H. Fish, H. S. Kim, R. H. Fong, *Organometallics* **1989**, *8*, 1375–1377.
[39] R. H. Fish, H. S. Kim, R. H. Fong, *Organometallics* **1998**, *10*, 770–777.
[40] J. Sandström, *Dynamic NMR Spectroscopy*, Academic Press, London, **1982**.
[41] H. M. P. Budzelaar, *gNMR*, version 4.1.0., Cherwell Scientific, Oxford, **1999**.
[42] M. L. H. Green, A. K. Hugues, *J. Chem. Soc., Dalton Trans.* **1992**, 527–536.
[43] C. L. Perrin, T. J. Dwyer, *Chem. Rev.* **1990**, *90*, 935–967.
[44] S. C. Dunn, P. Mountford, D. A. Robson, *J. Chem. Soc., Dalton Trans.* **1997**, 293–304.
[45] E. Rotondo, G. Bruschetta, G. Bruno, A. Rotondo, M. L. Di Pietro, M. Cusumano, *Eur. J. Inorg. Chem.* **2003**, 2612–2618.

[46] A. Rotondo, G. Bruno, M. Cusumano, E. Rotondo, *Inorg. Chim. Acta* **2009**, *362*, 4767–4773.
[47] A. Rotondo, *Inorg. Chem. Commun.* **2010**, *13*, 941–944.
[48] V. P. Fedin, A. G. Sykes, *Inorg. Synth.* **2002**, *33*, 162–170.
[49] M. N. Sokolov, R. Henández-Molina, D. N. Dybtsev, E. V. Chubarova, S. F. Solodovnikov, N. V. Pervukhina, C. Vicent, R. Llusar, V. Fedin, *Z. Anorg. Allg. Chem.* **2002**, *628*, 2335–2339.
[50] *VnmrJ*, 1.1 C, Varian Inc., **2003**.
[51] *COLLECT Program Suite*, Bruker Nonius, Delft, The Netherlands, **1997**–**2000**.
[52] Z. M. Otwinowski, W. Minor, "Processing of X-ray Diffraction Data Collected in Oscillation Mode" in *Methods in Enzymology*, vol. 276 (Macromolecular Crystallography, Part A) (Eds.: C. W. Carter Jr., R. M. Sweet), Academic Press, New York, **1997**, pp. 307–326.
[53] A. L. Spek, *Acta Crystallogr., Sect. A* **1990**, *46*, C34.
[54] *Sir2004: An improved tool for crystal structure determination and refinement*: M. C. Burla, R. Caliandro, M. Camalli, B. Carrozzini, G. L. Cascarazo, L. De Caro, C. Giacovazzo, G. Polidori, R. Spagna, *J. Appl. Crystallogr.* **2005**, *38*, 381–388.
[55] G. M. Sheldrick, *SHELXL-97, Program for the refinement of Crystal Structures*, University of Göttingen, Göttingen, **1997**.

Received: July 22, 2010
Published Online: January 5, 2011

